JOURNAL OF VIROLOGY, Aug. 1976, p. 620-636

Vol. 19, No. 2
Printed in U.S.A.

Early Events in Polyoma Virus Infection: Attachment, Penetration, and Nuclear Entry[1]

ROBERT L. MACKAY AND RICHARD A. CONSIGLI*
Division of Biology, Kansas State University, Manhattan, Kansas 66506

Received for publication 29 March 1976

The plaque-assay technique was used as a tool to determine the optimal conditions for adsorption of polyoma virions to host cells. Using these optimal conditions of adsorption, an electron microscopy study of the early events of infection was performed. By electron microscopy and autoradiography, it was demonstrated that both the viral coat proteins and DNA arrive simultaneously in the nucleus as early as 15 min postinfection. When horseradish peroxidase-labeled virions, pseudovirions, and capsids were used to infect cells, only the particles with nucleic acid or a factor(s) associated with the nucleic acid, i.e., histones, appeared to enter the nucleus. Moreover, when virions were used to infect either permissive or nonpermissive cells, identical early events of viral infection, i.e., adsorption, penetration, and nuclear transport, were observed, suggesting that these early events of infection are a property of the virion and not the host cell.

The early events of viral infection, from the time of viral attachment to the cellular receptor site to the time of viral DNA replication, can be broadly divided into two stages. The first stage are those events related to the interaction of the viral particles with the host cell, i.e., attachment, penetration, and uncoating (3, 10, 30). The second stage are those events related to the decoding of the viral genetic information, i.e., transcription and translation, and possible derepression of certain host regulatory systems resulting in subsequent modification of cellular or viral constituents (45). Although there is a wealth of information about polyoma virus-specific DNA, RNA, and protein synthesis in both permissive and nonpermissive host cells (42), very little is actually known about the early events of attachment, penetration, and uncoating in relation to the role that they play in determining whether a permissive or nonpermissive infection will result.

Polyoma virus can interact with cells in two distinct ways. The first interaction, a productive infection, results when the virus replicates in the cell nucleus, forming progeny virus particles, and subsequently kills the host cell (7, 35). Secondly, a nonproductive interaction can occur in which progeny virus are not produced and the host cells survive and acquire new properties like malignant cells (29, 36, 40, 44). Whether a cell undergoes a productive or nonproductive infection largely depends on the species of cells being infected. For example, mouse cells primarily undergo a productive or lytic infection, although they are capable of undergoing transformation at a low frequency. Rat or hamster cells, on the other hand, undergo transformation with a much higher frequency. Thus, although both productive and nonproductive responses may occur in cells of a given species, the response at the cellular level is mutually exclusive, i.e., the virus either replicates in or transforms the host cell (1).

The morphological aspects of the uptake of polyoma virus in cells are well documented (10, 30). However, the subsequent events, i.e., the site and mode of viral uncoating, have yet to be determined. Light (18) and electron (E. de-Harven, E. Borenfreund, and A. Bendich, Fed. Proc. 24:309, 1965) microscopy autoradiography studies suggest that the virion coat proteins are removed in the cytoplasm and only the viral genome enters the nucleus. Direct electron microscopy visualization of the virus suggests that the virus uncoats between the nuclear membranes (30), whereas biochemical fractionation studies (3) suggest that it reaches the nucleus intact, implying that uncoating occurs within the nucleus. These early studies, however, were performed at a time before there was an awareness of the defective and pseudovirion subpopulations of polyoma virus and with the use of suboptimal conditions of infection, which could have obscured the fate of the infecting virions. To overcome these difficulties, the

[1] Contribution no. 1272-J, Kansas Agricultural Experiment Station, Kansas State University.

present study was undertaken to determine optimal conditions of viral adsorption. Using these optimal conditions, purified polyoma virus subpopulations, virions, pseudovirions, and capsids, along with various ultrastructural tracers, were used to localize the virus during the early events of infection in both permissive and nonpermissive host cells.

(A preliminary report of this work was presented at the 75th annual meeting of the American Society for Microbiology, New York, N.Y., 1975.)

MATERIALS AND METHODS

Virus, cells, and media. Wild-type (large and small plaque) polyoma virus was originally obtained from Sarah Stewart, National Institutes of Health. Cells were obtained as follows: BALB/3T3 (Walter Eckhart, The Salk Institute), Py-3T3 (non-virus producing, Howard Green, New York University School of Medicine), BHK-21 (ATCC no. CCL-10), Py-BHK (non-virus producing, Claudio Basilico, New York University School of Medicine), and primary mouse embryo and primary baby mouse kidney cells from our own colony (COBS, CD-1, Charles River Mouse Farms). The growth and maintenance of primary mouse embryo cultures have been described previously (19). Primary baby mouse kidney, BALB/3T3, BHK-21, and Py-BHK were all propagated in Dulbecco modified Eagle medium (DME; GIBCO) supplemented with 10% heat-inactivated fetal calf serum.

Propagation of polyoma virus. Polyoma virus stocks were enriched in infectious virus by plaque isolation followed by two successive passages through newborn mice. Enriched stocks were maintained by passage at low multiplicity (less than 10 PFU/cell) on primary mouse kidney cells. Primary mouse kidney cells were grown in roller bottles in DME buffered with 40 mM HEPES buffer (Calbiochem) (38). Heat-inactivated fetal calf serum (10%) was added to the medium for cell growth but was absent for virus production. The virus was harvested at approximately 72 h after infection and purified as described below.

Preparation of radioisotopically labeled virus. Infected primary baby mouse kidney cultures were maintained in serum-free DME containing 20 μCi of [^{3}H]thymidine per ml of medium (ICN, 83.8 Ci/mmol) plus 8 μCi of [^{3}H]deoxycytidine per ml of medium (Schwarz/Mann, 25 Ci/mmol) to label the viral DNA. Other infected cultures maintained in DME containing 10% concentration of amino acids with 10 μCi of ^{3}H-labeled reconstituted protein hydrolysate per ml of media (Schwarz/Mann) were used to label the virion coat proteins. The virus was harvested at approximately 72 h after infection and purified.

Purification of polyoma virus. The purification of polyoma virus has been described previously (R. Consigli, J. Zabielski, and R. Weil, submitted for publication) and modified as follows. The infected cell lysate was centrifuged at 10,000 $\times$ g for 30 min. Virus remaining in the supernate was concentrated with polyethylene glycol as described by Friedmann and Haas (12). The pellet was suspended in Tris buffer (0.01 M, pH 7.4) and dispersed with a Sorvall Omnimixer. Receptor-destroying enzyme (Microbiological Associates) was added to 50 units/ml and the mixture was stirred at 37°C for 4 h. A sodium deoxycholate solution (0.5% DOC-0.1 M Tris buffer, pH 9.5) was added, and the mixture was stirred overnight at 4°C. Cellular debris was removed and extracted with Freon 113 (DuPont) according to Girardi (14), and the aqueous phases were pooled with the other cell-free viral supernates. The combined supernates were layered over 4 ml of 20% sucrose and centrifuged in a Spinco SW27 rotor at 25,000 rpm for 3 h. The pelleted virus was suspended in a minimal volume of Tris buffer (0.01 M, pH 7.4), layered over a preformed CsCl gradient (1.25 to 1.35 g/cm^3), and centrifuged to equilibrium in an SW50.1 rotor at 35,000 rpm for 16 h. Two discrete virus bands were observed; complete virus (bouyant density, 1.32 to 1.33 g/cm^3) and capsids (bouyant density, 1.28 to 1.29 g/cm^3). They were individually collected and dialyzed against Tris buffer (0.01 M, pH 7.4). The respective preparations were layered over a preformed velocity CsCl gradient (1.27 to 1.35 g/cm^3) and centrifuged in an SW50.1 rotor at 35,000 rpm for 2.5 h. Gradients were fractionated, and the appropriate fractions of virions, light pseudovirions, and capsids were respectively pooled and dialyzed first against Tris buffer (0.01 M, pH 7.4) and then against Puck saline G (PSG) (34).

Determination of optimal conditions of viral adsorption. The optimal conditions for virion adsorption were determined using the plaque assay technique (6). A polyoma virus stock was diluted to yield 50 to 60 plaques per 60-mm culture dish of primary mouse embryo fibroblasts.

To determine the optimal temperature of viral adsorption, cells and virus dilutions were equilibrated at various temperatures over a range from 4°C to 40°C for 20 min prior to infection. The virus was allowed to adsorb for 3 h at the respective temperature, unadsorbed virus was removed, the cells were washed twice at the respective temperature with PSG, and plaque medium was added.

The optimum pH of viral adsorption was determined by equilibrating cells for 20 min prior to infection in DME media at 37°C buffered with Tris-acetate buffer (0.026 M) over the pH range of 6.0 to 8.5. Virus stock was diluted in the respective pH media and allowed to adsorb for 3 h, unadsorbed virus was removed, the cultures were washed with DME of the respective pH, and plaque medium was added.

The optimal time of virus adsorption was determined by infecting cells at 36°C and pH 7.4, unadsorbed virus was removed at various intervals, cultures were washed with PSG, and plaque media were added at various times postinfection.

The integrity (susceptibility to nuclease) of the virion crossing the cell membrane was determined by plaquing in the presence of either pancreatic DNase (200 μg/ml; Calbiochem) with 10^{-3} M $MgCl_2$ or snake venom phosphodiesterase (160 μg/ml;

Worthington) with 10^{-3} M $MgCl_2$ or in the presence of both enzymes. Activity of the commercial enzyme was confirmed using radioactively labeled bacteriophage T_7 DNA (a gift of Melvin S. Center) as a substrate.

Preparation of horseradish peroxidase-labeled antibodies to polyoma virus structural proteins. Antibodies to various purified polyoma virus proteins were prepared as follows. Purified polyoma virions were disrupted by boiling for 5 min in sodium dodecyl sulfate (SDS) (2%) and 2-mercaptoethanol (5%). Viral capsomeres were prepared as described previously (R. Consigli, J. Zabielski, and R. Weil, submitted for publication) using carbonate-bicarbonate buffer (0.1 M, pH 10.5) at 25°C for 60 min followed by the addition of dithiothreitol (5×10^{-3} M), EDTA (10^{-3} M), and NaCl (0.2 M) for an additional 1 h. Antibodies to polyoma virions, capsomeres, and SDS-disrupted virions were prepared in rabbits.

The monovalent Fab' antibody fragments were isolated from whole serum according to the method of Madsen and Rodkey (J. Immunol. Methods, in press) using a column of LKB AcA 34 Ultrogel. Antibody protein determinations were performed according to Steiner and Lowey (39). Horseradish peroxidase (type VI) was conjugated to antibody fragments by the method of Nakane and Kawaoi (33).

Radioimmunoprecipitation of virus particles reisolated from infected cells. Confluent monolayers of primary baby mouse kidney cells were infected with purified ^{3}H-amino acid-labeled polyoma virions. One group of cells was infected at 4°C to allow attachment but not penetration, and another was infected at 37°C to allow both attachment and penetration. After 3 h, unadsorbed virus was removed, and virus particles that had attached but not penetrated were removed by treating the cells with receptor-destroying enzyme (100 units/ml) and high pH (Tris buffer, 0.1 M, pH 9.5) for 1 h. Unlabeled carrier virus was added to each preparation, and the virus was purified from both the 4°C and 37°C cultures as described above, except that both the Freon 113 and sodium deoxycholate extraction steps were omitted. After equilibrium CsCl gradient centrifugation, fractions were collected and assayed for both radioactivity and hemagglutination activity. The bouyant density of the peak fractions was determined and compared to the stock purified control polyoma virus. Appropriate fractions were then pooled and dialyzed against Tris buffer (0.01 M, pH 7.4) and examined by negative-stain electron microscopy. Indirect radioimmunoprecipitation was performed on the 4°C and 37°C reisolated virus and control virus according to the procedure of Horwitz and Scharff (16). The immunoglobulin G fraction of rabbit antipolyoma virion antiserum was purified from whole serum by the technique of Kekwick (17) followed by chromatography on DEAE-cellulose according to Levy and Sober (22). The optimal proportion of both the rabbit antipolyoma virus immunoglobulin G and the virion protein were first determined, and then the assay was performed on the respective ^{3}H-labeled virus samples, each containing 10 μg of viral protein.

Electron microscopy techniques. For thin-section electron microscopy studies, cells were washed twice with PSG and infected with saturating concentrations (1,000 to 5,000 PFU/cell) of purified virus in a minimal volume to enhance virus-cell contact. Virus was allowed to adsorb with occasional redistribution of the inoculum. Unadsorbed virus was removed, monolayers were washed with PSG, and medium was added. Cells were harvested at the appropriate times by washing once with PSG and fixed at 4°C for 1 h in 3% glutaraldehyde in cacodylate buffer (0.05 M, pH 7.4). The fixed cells were washed with PSG, scraped from the dish with a rubber wedge, and gently pelleted and postfixed in 1% osmium tetroxide in the phosphate buffer of Millonig (31). The fixed cells were embedded in Epon 812 according to the procedure of Luft (25), and ultrathin sections were cut with a diamond knife (DuPont) using an LKB Ultratome III microtome.

For electron microscopy autoradiography studies, ^{3}H-DNA-labeled polyoma virions and ^{3}H-coat protein-labeled virions were each used to infect a set of primary baby mouse kidney cultures. Unadsorbed virus was removed at 3 h postinfection, and fresh DME medium was added. At appropriate times after infection, cultures were fixed and embedded as above. Autoradiography was performed by the method of Kopriwa (21) using Ilford L-4 emulsion. For grain localization and distribution studies, the radioautographs were developed using the chemical developer D-19b (21). For fine-grain development, high-resolution studies, gold latensification in conjunction with the Agfa-Gevaert physical developer of Kopriwa (21) was used.

For the enzyme-labeled antibody studies, cells were fixed with 1% formaldehyde in phosphate buffer (0.05 M, pH 7.4) with 4% sucrose. The fixed cells were washed with PSG, equilibrated by the freezing media of Nakane (32), and then rapidly frozen, thawed, and washed, and the appropriate enzyme-labeled antibody conjugate was added. The electron-dense deposit was developed with 3,3'-diaminobenzidine (Sigma) by the procedure of Graham and Karnovsky (15), and the cells were postfixed and embedded as above.

All specimens were examined and photographed in a Phillips 201 electron microscope, the magnification of which was calibrated with a carbon grating replica having 2,160 lines/mm (Fullam).

Preparation of horseradish perioxidase-labeled polyoma virus. For enzyme-labeled virus studies, purified polyoma virus was conjugated to horseradish peroxidase (type VI) (Sigma) using the technique of Nakane and Kawaoi (33). Plaque assays demonstrated a reduction of only 1 log of infectivity in virions that were conjugated to the enzyme. After conjugation the virus was separated into complete, pseudovirion, and capsids using the velocity CsCl gradients described earlier. Cells infected with these preparations were fixed with glutaraldehyde and washed with PSG, the electron-dense tracer was developed, and the cells were washed, postfixed, and embedded as above.

Quantitative assays. Radioactivity was quantitated in an aqueous toluene-based scintillation fluid (toluene-Triton X-100, 3:1) using a Beckman LS-233

liquid scintillation counter. Bouyant densities were determined with a Bausch & Lomb refractometer using the equation of Vinograd and Hearst (43). Hemagglutination techniques have been described previously (6). Protein determinations were by the method of Lowry et al. (24) using bovine serum albumin as the standard.

RESULTS

Optimal conditions of viral adsorption. The optimal conditions of viral adsorption are shown in Fig. 1. The optimal temperature of viral adsorption was found to be 37°C. Adsorption at 4°C, which resulted in attachment but not penetration, allowed approximately 90% of the virions to adsorb at 4°C when compared to 37°C (Fig. 1A). The optimal pH of viral adsorption (Fig. 1B) was pH 7.4, and the optimal time of viral adsorption (Fig. 1C) in PSG was 3 h. Fifty percent of the input virus was adsorbed in the initial 30 min of infection.

Preliminary experiments demonstrated that there is a Na^+ ion requirement for viral adsorption. Once the ion requirements were determined, the nutritional requirements of cells undergoing viral adsorption were examined. The data demonstrated that the nutritional requirements during the first 3 h of viral adsorption were not very stringent. After 3 h of viral adsorption, however, significant nutrient requirements were needed (data not shown). Consequently, for electron microscopy studies, Puck saline G, a buffer specifically designed for use with tissue-cultured cells (39), was used as the adsorption medium.

Electron microscopy autoradiography. Figures 2 (chemical development) and 3 (physical development) clearly demonstrate that the infecting virion DNA and coat proteins arrived simultaneously in the nucleus, as early as 15 min postinfection. Chemical development with D-19b produces large autoradiography grains but gives maximal sensitivity. Even under these low-resolution conditions where the half-distance for Ilford L-4 emulsion is reported to be 160 nm (37), both the ^3H-labeled viral DNA and ^3H-labeled viral coat protein-labeled virions produced grains that are clearly within the nucleus. Moreover, when the half-distance was decreased by using the high-resolution physical developer of somewhat lower sensitivity, the grains were again observed in the nucleus.

The distribution of grains in thin-sectioned cells with respect to time of infection is shown in Table 1. In both the ^3H-virion DNA-labeled and ^3H-virion-labeled coat protein infected cells, the total number of grains increased with time of adsorption and then plateaued at 3 h postinfection, when the inoculum was removed and replaced with media. Parallel grain distribution percentages with time were obtained with both radioisotopically labeled DNA and coat protein preparations, again suggesting that both components arrive simultaneously in the nucleus for subsequent uncoating.

The distribution of the labeled virions in the cell changed remarkably with time. Although grains were localized in the nucleus as early as 15 min postinfection, the majority of the grains, i.e., virus particles, were localized at the cell

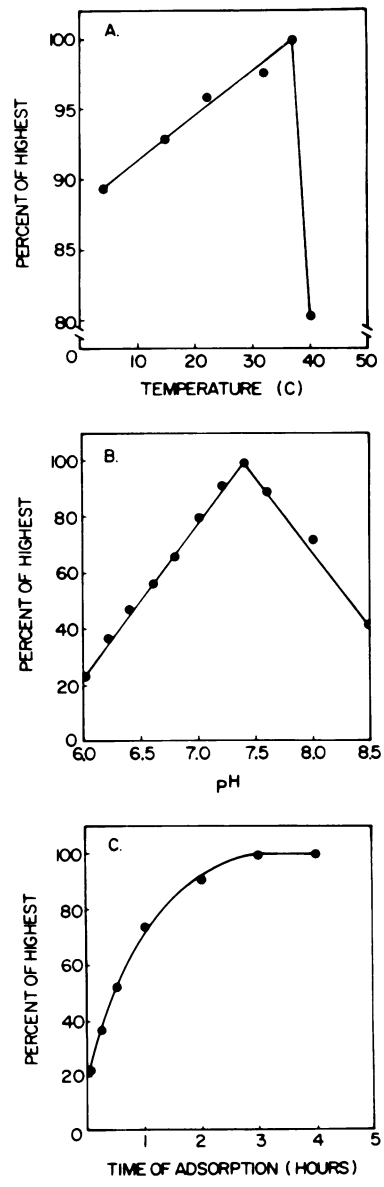

FIG. 1. *Optimal conditions of viral adsorption as determined by the plaque assay technique. (A) Temperature, (B) pH, and (C) time of adsorption.*

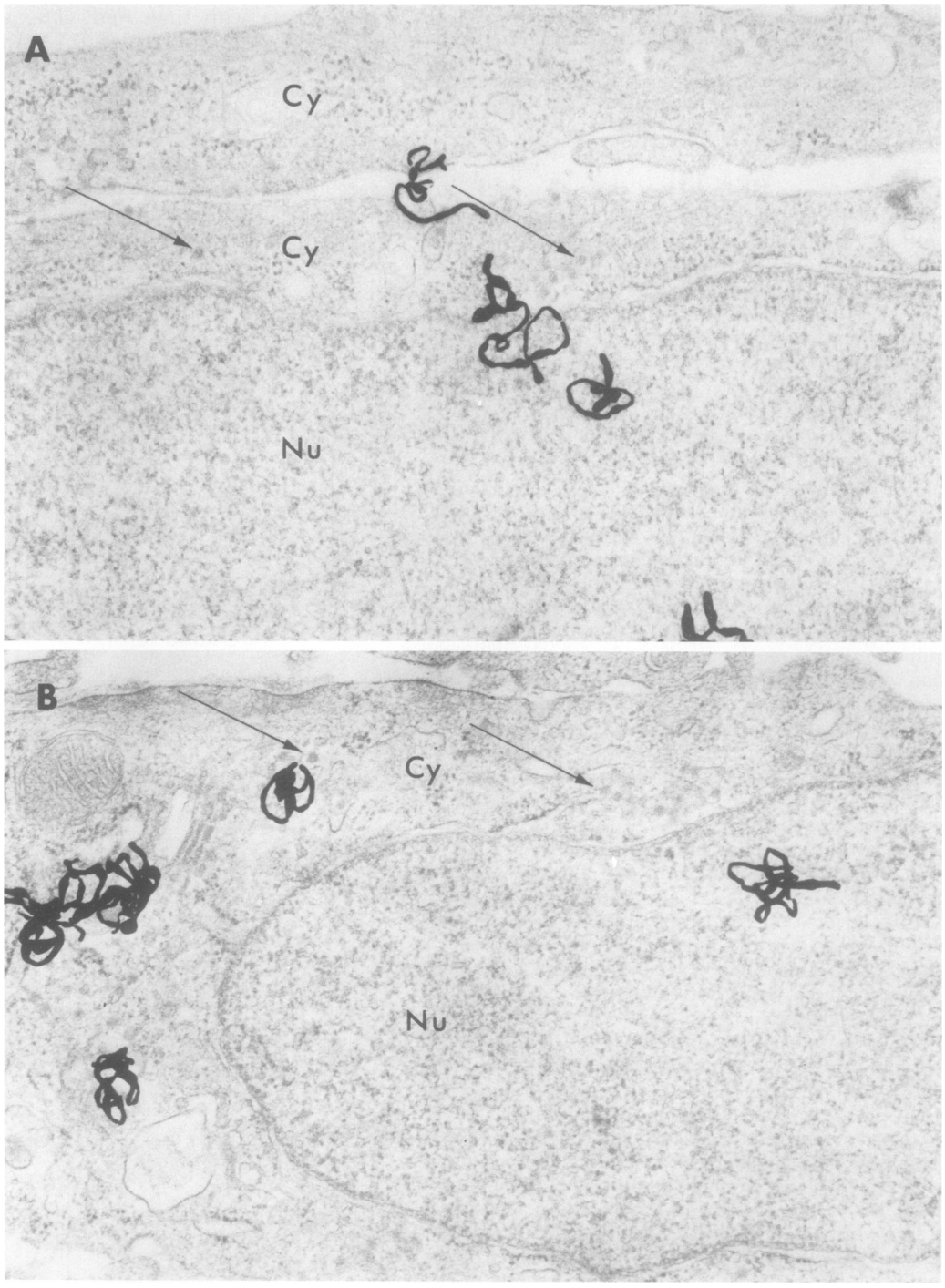

FIG. 2. *Electron microscopy autoradiography of thin-sectioned primary baby mouse kidney cells at 15 min postinfection using ^{3}H-labeled polyoma virions. Plates were developed for maximal grain sensitivity with a chemical D-19b developer. (A) ^{3}H-DNA-labeled virions; (B) ^{3}H-amino acid-labeled virions. Non-grain-producing virus can also be seen (arrows). The designations Nu for nucleus and Cy for cytoplasm are used in this and subsequent micrographs. ×37,750.*

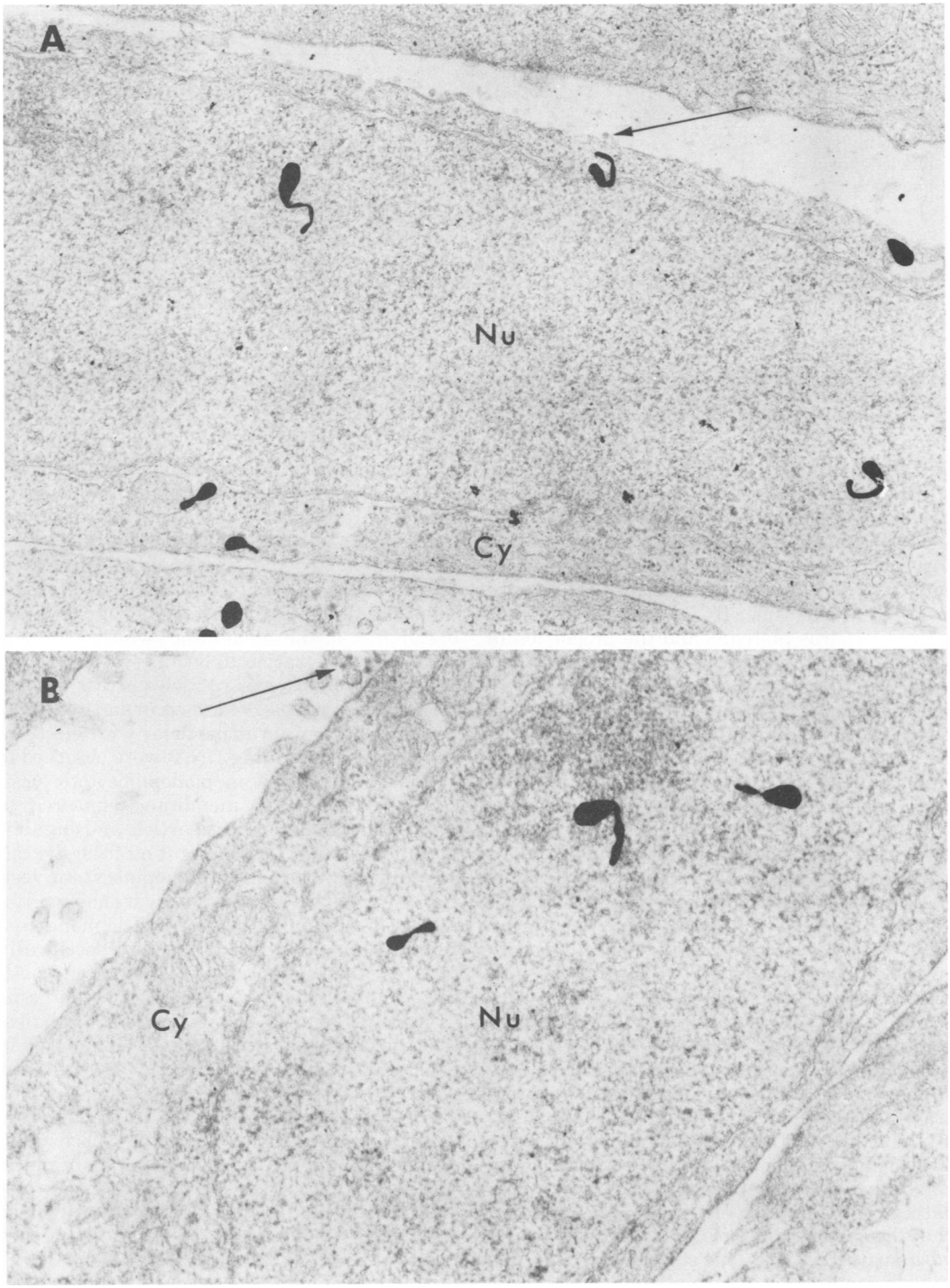

FIG. 3. *Electron microscopy autoradiography of thin-sectioned primary baby mouse kidney cells at 15 min postinfection using ^{3}H-labeled polyoma virions. Developed for high resolution with the physical developer. (A) ^{3}H-DNA-labeled virions; (B) ^{3}H-amino acid-labeled virions. Arrows point to non-grain-producing virions. ×37,750.*

TABLE 1. *Autoradiography of ^{3}H-labeled virion DNA and coat protein infected cells*

	Time post-infection (h)	Total grains counted[a]	Maximal grains adsorbed (%)	Total grains counted (%) over:				
				Cell surface	Cytoplasm	Perinuclear	Nucleus	Non-cell associated[b]
Radioactively labeled virion DNA	0.25	238	26	44.96	46.22	5.46	2.10	1.26
	1	400	44	32.00	51.00	7.25	8.75	1.00
	3	949	100	16.54	57.43	9.27	16.12	0.65
	6	910	100	9.45	49.01	13.96	26.70	0.88
	10	896	100	5.36	33.92	19.98	40.18	0.56
Radioactively labeled virion coat proteins	0.25	97	33	47.42	41.24	8.25	3.09	0.00
	1	149	51	33.55	44.97	9.40	11.41	0.67
	3	308	100	13.96	58.77	10.39	15.58	1.29
	6	299	100	8.03	50.84	14.38	25.75	1.00
	10	282	100	7.45	31.21	21.99	37.94	1.41

[a] Total grains counted over 25 randomly selected cells.
[b] Noncellular associated or background grains.

surface at this early time. By 1 h postinfection, the distribution of virus at the cell surface was decreasing, whereas that in the cytoplasm was increasing, suggesting that the majority of the virus was migrating into the cytoplasm. The proportion of virus in the nucleus was also increasing at this time. By 3 h postinfection, the uptake of virus plateaus and the proportion of virus in the cytoplasm reached a maximum and then began to decrease, concomitant with an increase in grains in the nucleus. Grains were observed to accumulate with time, at the same percentage level, in the nucleus of infected cells in both the DNA and coat protein-labeled virions. Non-cell-associated or background grains observed remained at a small (less than 1%) and relatively constant percentage (Table 1).

Electron microscopy of viral attachment, penetration, and uncoating. Since autoradiography studies demonstrated that the virion DNA and coat proteins arrive simultaneously in the nucleus as early as 15 min under optimum conditions of adsorption, attempts were made to directly visualize these events in the electron microscope.

Figure 4 demonstrates the sequence of events of polyoma virion attachment, penetration, and transport to the nucleus. Attachment studies at 4°C demonstrated that virus particles were able to attach but not penetrate the cell under these conditions. Infection of cells at 4°C, using saturating concentrations of virions, demonstrated that the entire surface of the cell can be covered with virus particles. This suggests that the cellular receptor sites are evenly distributed over the surface and are not relegated to one particular area of the cell surface (data not shown). At 4°C virus particles were observed to undergo either a loose (Fig. 4A) or a tight (Fig. 4B) interaction with the cellular receptor site.

Virus particles that were allowed to adsorb at 37°C underwent both attachment and penetration. Figure 4C shows a group of virus particles that appear to be attached very tightly to the cell surface, and the membrane appears to be slightly depressed beneath the virus particle. Thus the final stage of attachment may be an undulation of the membrane, which acts as a signal for penetration to begin.

Penetration of virus particles across the cell membrane was observed to occur in two forms. In the first form virus particles with electron-dense cores (containing DNA) were observed to enter the cytoplasm in monopinocytotic vesicles. Next, the cell membrane appeared to tightly surround the virus particle and engulf it into the cytoplasm, pinching it off from the cell membrane and forming a monopinocytotic vesicle. The events of penetration by monopinocytosis are shown in Fig. 4D and E. The monopinocytotic vesicle appears to migrate specifically towards the outer nuclear membrane. Although attachment and penetration can occur in areas of microfilaments and microtubules, these structures do not appear to be involved in the transport of the virus particle to the outer nuclear membrane (data not shown). Virus particles were next observed in the nucleus devoid of a membrane. The actual mechanism of passage through the nuclear membrane is obscure. It is possible that the membrane around the virion fused with the outer nuclear membrane at a site other than the nuclear pore complex, and only the virions proceeded into the nucleus (Fig. 4F). Virus particles were not observed to accumulate in the nucleus and thus are presumed to be rapidly uncoated.

The second form of penetration was one in which virus particles with transparent cores (devoid of DNA) were observed to enter the

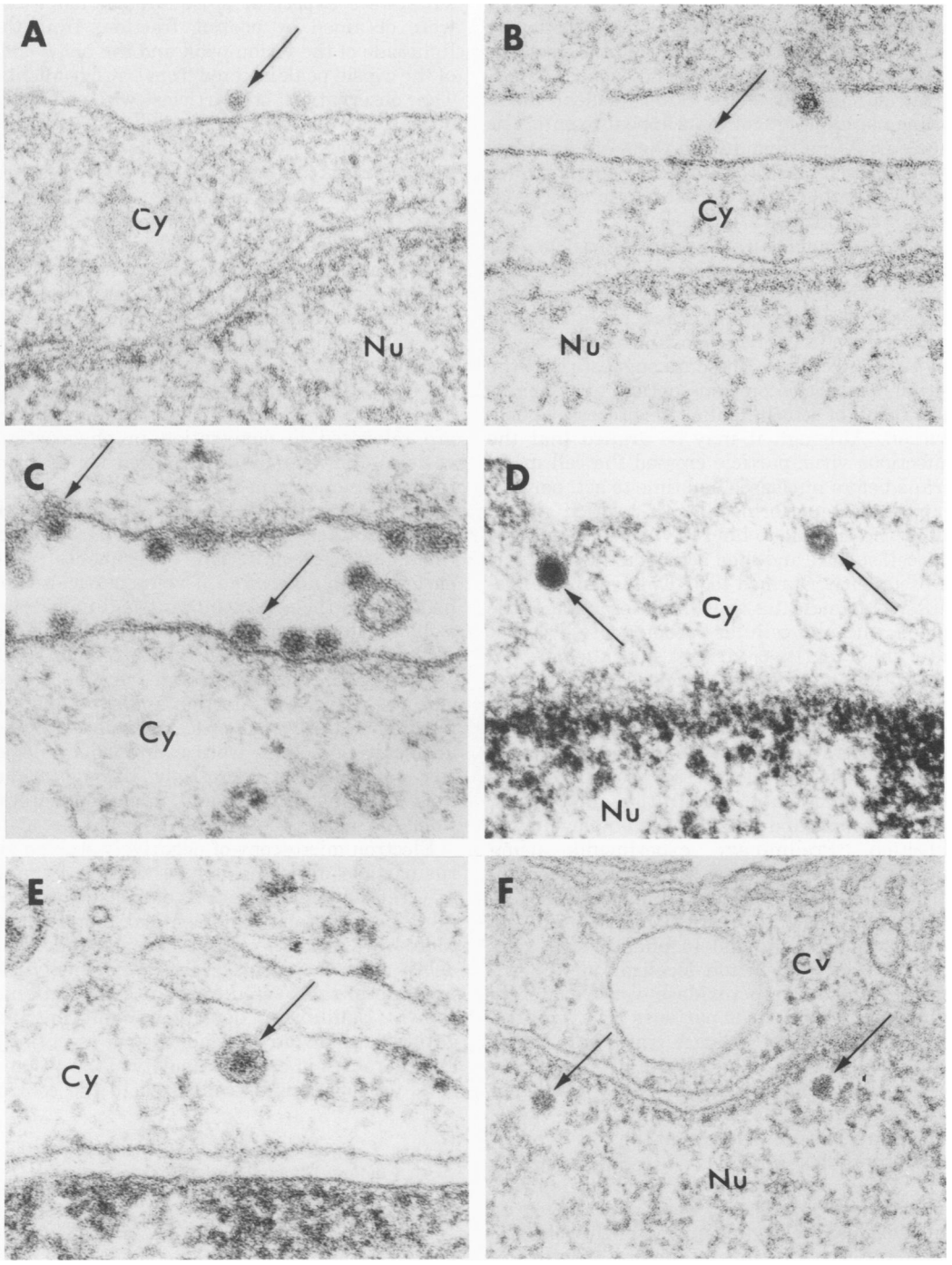

FIG. 4. *Attachment, penetration, and nuclear transport sequence of polyoma virions. (A) Loose interaction of virion (arrow) with a cellular receptor site; (B) tight interaction of virion (arrow) with the cellular receptor site; (C) tight interaction of virions (arrows) with the cellular receptor site; (D) penetration of virions (arrows) into monopinocytotic vesicles; (E) migration of virion in monopinocytotic vesicle (arrow) towards the outer nuclear membrane; (F) intact virions (arrows) in the nucleus. ×88,850.*

cytoplasm in large membrane-enclosed groups much like phagocytotic vesicles. A few virus particles with dense cores were fortuitously trapped within these phagocytotic vesicles. However, these vesicles did not appear to migrate specifically to the outer nuclear membrane nor did their contents appear to enter the nucleus. At no time during these studies were virus particles with electron transparent cores observed either in monopinocytotic vesicles or within the nucleus.

Effect of nucleases on viral infectivity. Experiments were also performed to determine if virion attachment and penetration altered the integrity of the infecting virion. Table 2 demonstrates the effect of both exo- and endonucleases on viral infectivity. The data suggests that the virion does not become susceptible to nucleases as a result of attachment or the process of penetration. Although it may be argued that the infectious virus particle crossed the cell membrane before nucleases had time to act, parallel experiments performed at 4°C, which should allow the enzyme to bind to virions attached to the cell surface and then act when the culture is subsequently warmed to 37°C, gave similar results. This indicates that the interaction of the virion with the cellular receptor site does not alter the integrity of virions, since they are not susceptible to exogenous nucleases.

Fate of virion, pseudovirion, and capsids in permissive cells. Since two mechanisms of viral penetration appear to be operative with polyoma virus, it was necessary to differentiate which mechanism of penetration the virions, pseudovirions, and capsids each employ during infection. Preliminary experiments using highly purified virions and capsids demonstrated sharp differences. Virions were observed to penetrate by monopinocytosis, and capsids entered the cell in phagocytotic vesicles. To facilitate virion localization, the enzyme horseradish peroxidase was covalently conjugated to the virus particles prior to infection, and the electron-dense tracer was subsequently developed. The results using virions, pseudovirions, and capsids labeled with the enzyme as a tracer are shown in Fig. 5.

Polyoma capsids penetrated the cell in phagocytotic vesicles (Fig. 5A). The complete virions (Fig. 5B) were observed to enter the cytoplasm by monopinocytosis and then migrate to the outer nuclear membrane and enter the nucleus. These observations are in agreement with the results using direct visualization of the virus (Fig. 4F).

The penetration of pseudovirions (Fig. 5C) proved to be a combination of entry in monopinocytotic and phagocytotic vesicles. These results were expected, since the pseudovirions were obtained by pooling fractions from the light side of the virion peak and the heavy side of the capsid peak isolated from CsCl gradients. The observation of particles with electron-dense cores in the nucleus indicates that the pseudovirions enter the nucleus by a mechanism similar to that observed for infectious virions. Thus the monopinocytotic form of penetration appears to be reserved for nuclear transport of virions and pseudovirions. This data suggests that there is a nuclear transport recognition factor(s) present on virions and pseudovirions that is recognized by the cellular receptor site as a possible signal to undergo the monopinocytotic form of penetration, thereby insuring nuclear transport and entry. Capsids, on the other hand, must lack this factor(s) and hence are relegated to penetration in phagocytotic vesicles and are possibly marked for destruction or removal from the cell.

Antigenic characterization of virus particles reisolated from infected cells. Indirect radioimmunoprecipitation experiments were performed to determine if virus particles that had crossed the cell membrane had undergone a change in antigenicity. ^{3}H-amino acid-labeled virions were used to infect cells at 4°C and 37°C. Virus particles were reisolated from infected cultures at 3 h postinfection and subsequently purified on CsCl gradients. Their physical and antigenic properties were examined by negative-stain electron microscopy, hemagglutination, bouyant density, and immunoprecipitation.

Electron microscopy of negatively stained virus particles from the control and the 4°C and 37°C reisolated preparations demonstrated that all 3 preparations had identical morphology. Moreover, residual cell membranes and other debris were not observed in the purified virus preparations recovered from the cells (data not shown). Equilibrium density gradient centrifugation data (Table 3) demonstrated essentially no differences in bouyant density of the 4°C and 37°C preparations as compared to the control

TABLE 2. *Effect of exo- and endonucleases on the biological activity of adsorbed virus*

Treatment	Titer[a] (PFU/ml × 10^{8})
Control	3.20
Exonuclease	3.80
Endonuclease	3.80
Both	4.50

[a] Determined 3 h postinfection.

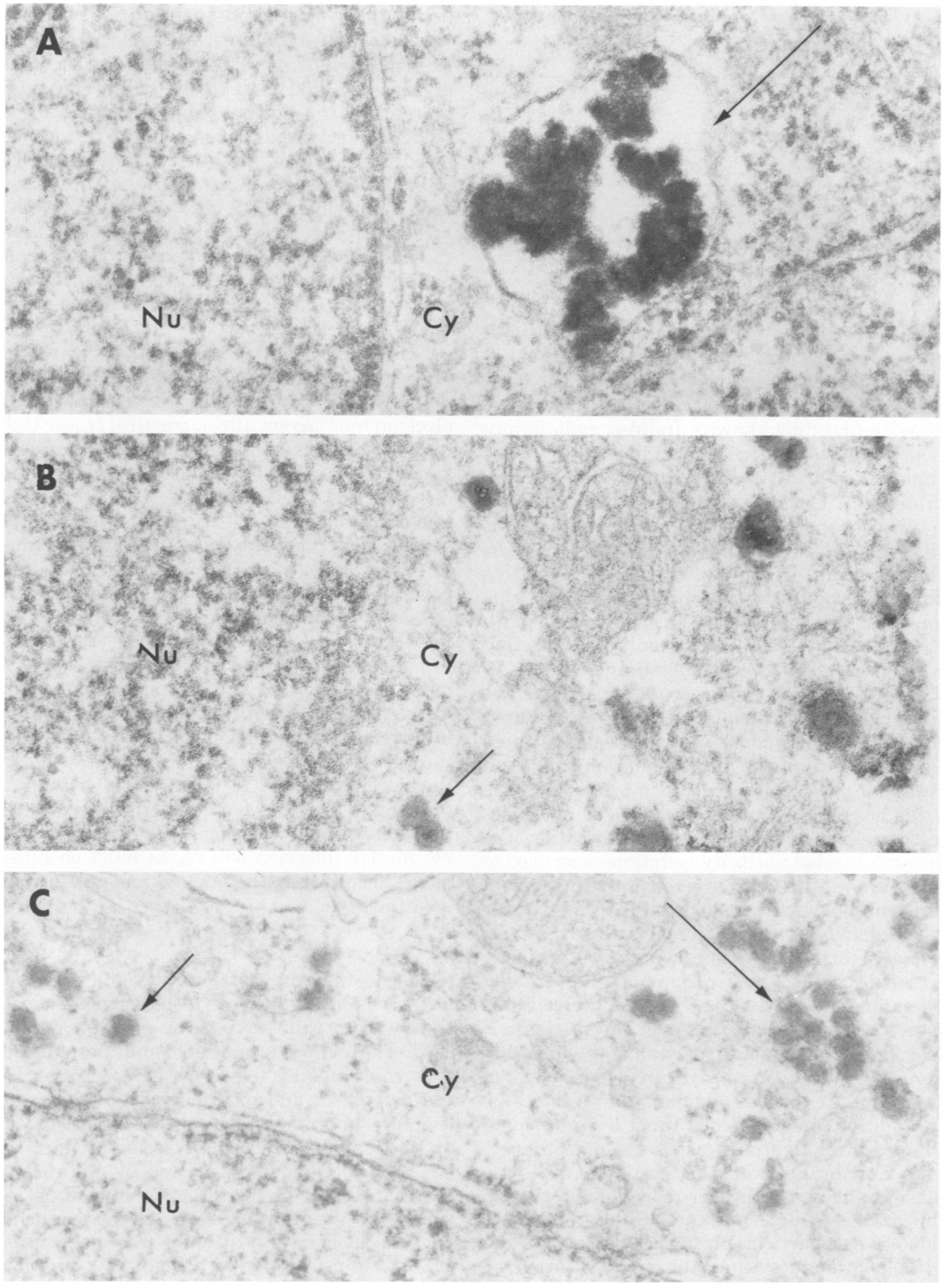

FIG. 5. *Horseradish peroxidase-labeled polyoma virus-infected primary baby mouse kidney cells at 3 h postinfection. (A) Polyoma virus capsids shown in groups in phagocytotic vesicles; (B) polyoma virions shown in monopinocytotic vesicles; (C) polyoma virus pseudovirions shown in both monopinocytotic vesicles (short arrows) and phagocytotic vesicles (long arrows). ×79,850.*

TABLE 3. *Bouyant density determination and radioimmunoprecipitation of virions reisolated from infected cells*

Virion sample	Density of reisolated peak (g/cm³)	cpm in:		Total cpm	Radioactivity (%) in:	
		Pellet	Supernate		Pellet	Supernate
Control	1.327	19,273	576	19,849	97.1	2.9
37°C[a]	1.320	5,307	338	5,645	94.0	6.0
4°C[a]	1.329	3,560	364	3,924	90.7	9.3

[a] Virions were reisolated 3 h postinfection.

virus, which was not allowed to interact with cells. Radioactivity and hemagglutination assays determined from the fractions of the CsCl gradients demonstrated coincidental peaks of activity (data not shown). Indirect radioimmunoprecipitation data is shown in Table 3. Virus that was allowed to penetrate the cell membrane at 37°C was recognized just as efficiently by the anti-polyoma virion antiserum as virus that was allowed to attach at 4°C or as the control virus. It may be concluded from this data that there is no significant change in virion morphology, density, antigenicity, or ability to hemagglutinate as a result of interacting with or crossing the cell membrane.

Integrity of the virions from the cell surface to the nucleus as seen by electron microscopy. Since radioimmunoprecipitation demonstrated that the virus is not altered antigenically as a result of crossing the cell membrane, and the virus does not become susceptible to nucleases as a result of attachment and penetration, the enzyme-labeled antibody technique was used to determine if the virus arrives in the nucleus in an immunologically recognizable form. The results shown in Fig. 6 demonstrate that the monovalent Fab' portion of the viral antibody molecule, which was coupled to horseradish peroxidase, localizes the virus on the cell surface, in the cytoplasm, and in the nucleus. It was found that the Fab' portion of the antibody molecule must be used to insure adequate penetration of the antibody conjugate into the cells. In addition, infected cells must be frozen and thawed after fixation to free the monopinocytotic membrane from the virion in the cytoplasm to allow the antiserum conjugate to bind the antigenic determinants. Similar localization of virus particles on the cell surface, in the cytoplasm, and within the nucleus occurred with antiserum to SDS-disrupted virions and to isolated capsomeres. This data further substantiates that the coat proteins do not undergo a loss of antigenicity as a result of attachment, penetration, and nuclear entry, since the purified antibody fragments to the various polyoma virus structural proteins, i.e., virions, SDS-disrupted virions, and capsomeres, were each able to recognize and bind to the virion structural proteins in the nucleus. However, this immunological technique revealed that virions entered the nucleus but were not found to accumulate. This was in contrast to the autoradiography experiment (Table 1) where virion DNA and coat proteins were found to accumulate in the nucleus with time of infection. Thus it may be concluded that the virus arrives intact in the nucleus and that uncoating is an event subsequent to nuclear entry.

Attachment, penetration, and nuclear entry of polyoma virions in various permissive and nonpermissive host cells. Since the various electron microscopy ultrastructural tracer techniques demonstrated that the virions arrive intact in the nucleus of primary baby mouse kidney cultures, it was of interest to determine if nuclear entry was a feature reserved for productive infection. The fate of purified polyoma infectious virions was then examined in other permissive, i.e., primary mouse embryo and BALB/3T3, and nonpermissive, i.e., BHK-21, Py-BHK, and Py-3T3, rodent cells. As seen in Fig. 7A–F, similar mechanisms of viral attachment, penetration, and virion nuclear entry were observed in both permissive and nonpermissive cells. This suggests that the outcome of the early events of virion attachment, penetration, and transport to the nucleus is solely a function of the virus particle. Thus the event(s) that determines whether a permissive or nonpermissive infection will result must be subsequent to entry into the nucleus and possibly is a host function.

DISCUSSION

Due to the small size of polyoma virus (45 nm), it is often difficult to positively identify the virus in thin sections by electron microscopy. There are a number of small normal cellular constituents, e.g., ribosomes, present in the cytoplasm and on the nuclear membrane that are approximately the same size as the virus. In addition, various fixation artifacts occur both in the cytoplasm and in the nucleus that can easily be mistaken for the virus. To overcome these difficulties, two approaches were used. First, an attempt was made to increase the probability of visualizing the virus by increasing the number of virus particles that entered cells. Second, various ultrastructural tracer techniques were used to positively identify the virus.

To increase the number of virus particles

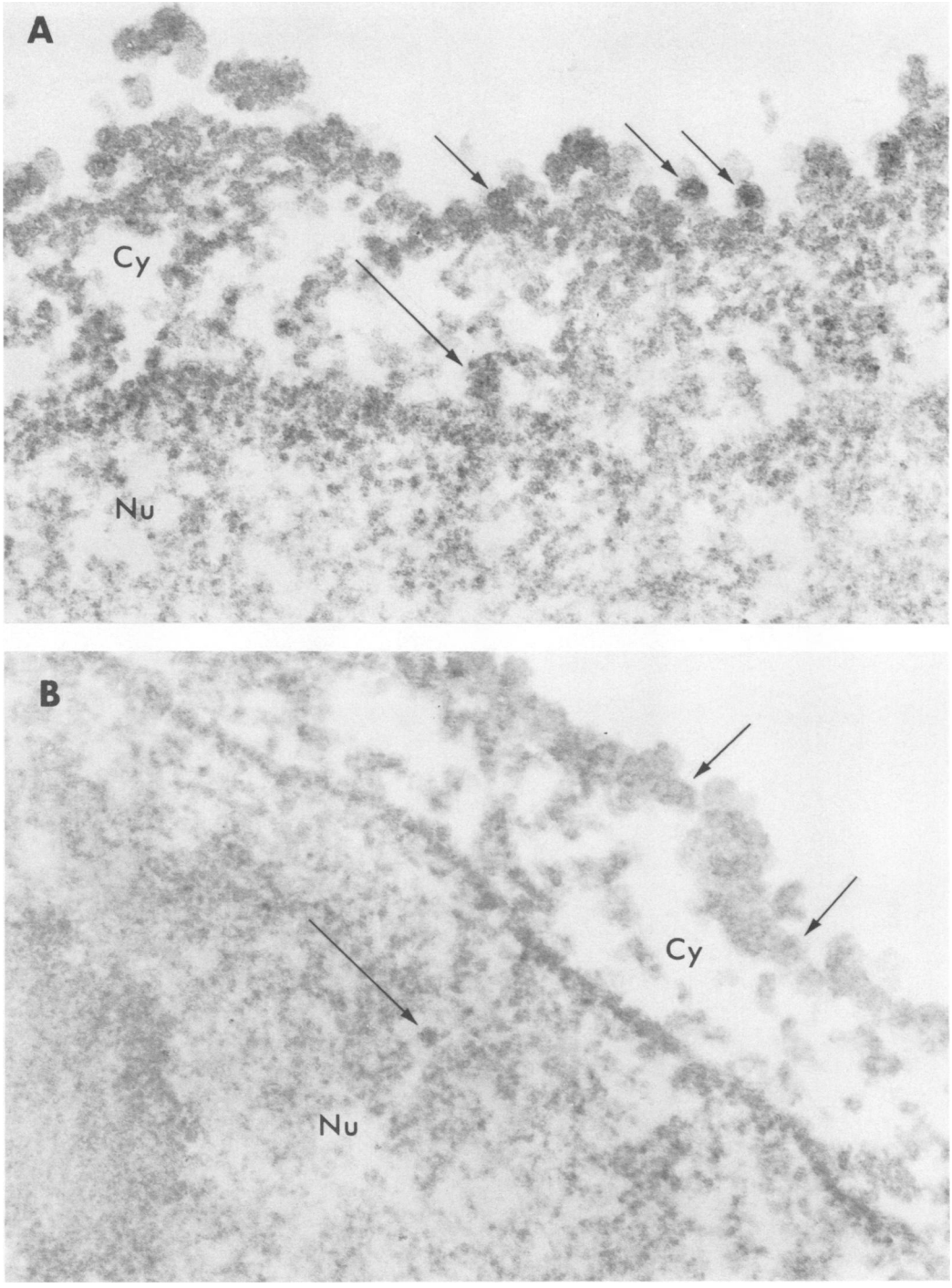

FIG. 6. *Localization of polyoma virions in thin sections of primary baby mouse kidney cells at 3 h postinfection using horseradish peroxidase-labeled Fab' antibody fragments to polyoma virions. (A) Polyoma virions attached to the cell surface (short arrows) and in a monopinocytotic vesicle in the cytoplasm (long arrows); (B) polyoma virions on the cell surface (short arrows) and within the nucleus (long arrow). ×71,900.*

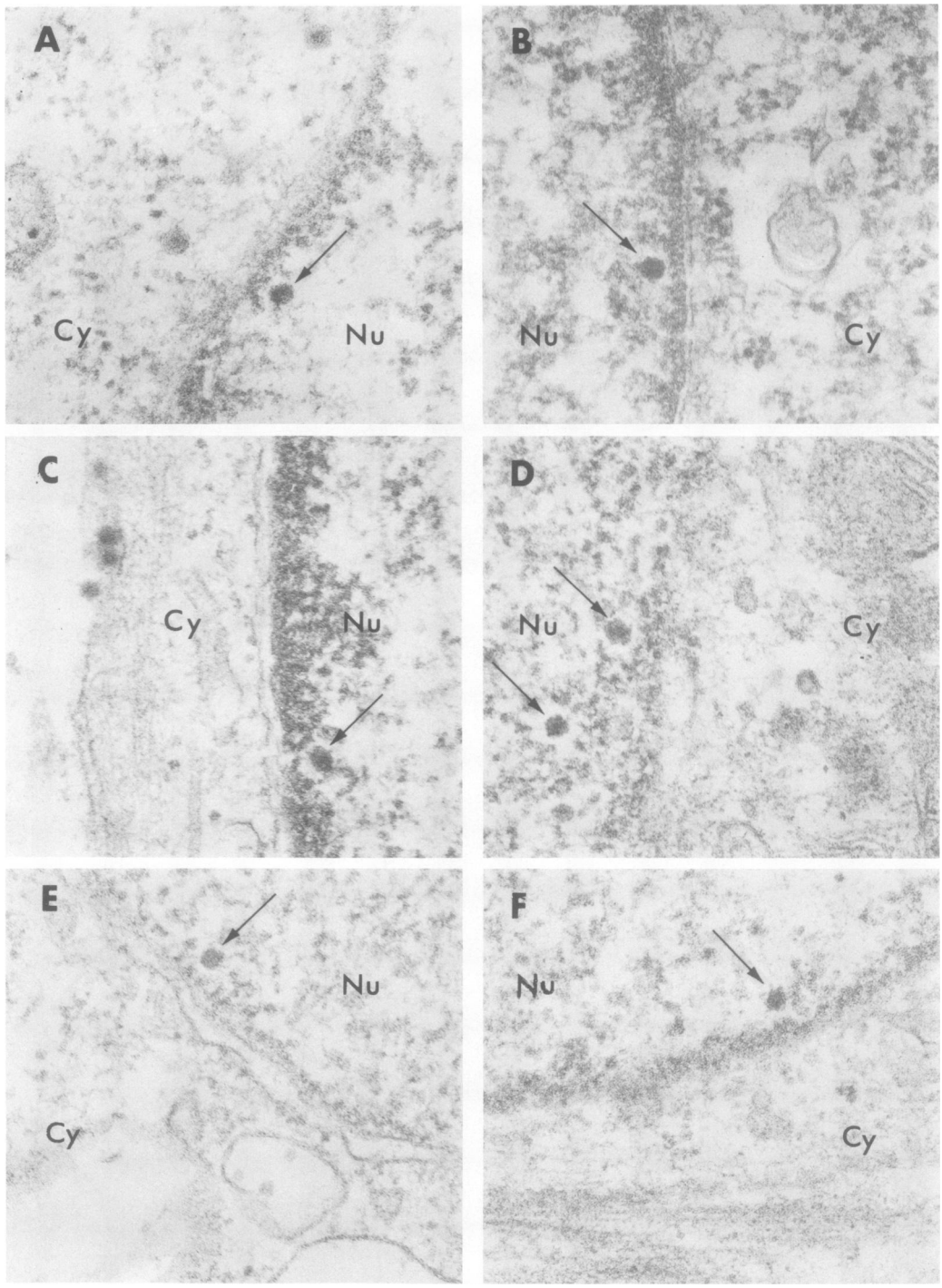

FIG. 7. *Polyoma virions in the nucleus of various permissive and nonpermissive rodent cells at 3 h after infection. (A) Primary mouse embryo; (B) primary baby mouse kidney; (C) BALB/3T3; (D) Py-3T3; (E) BHK-21; and (F) Py-BHK cultures. Arrows point to polyoma virions within the cell nucleus.* ×70,500.

that enter the cell, virus stocks were first enriched in infectious virus by plaque isolation. The optimal conditions of virion adsorption were determined (Fig. 1A–C), and saturating concentrations of virus particles were used to infect cells under these optimum conditions for electron microscopy studies. Three types of ultrastructural tracers were used. (i) Purified virions that were radioisotopically labeled in either the virion DNA or coat proteins were localized in infected cells by high-resolution electron microscopy autoradiography (Table 1). (ii) Subpopulations of polyoma virus (virions, pseudovirions, and capsids) were labeled with the enzyme horseradish peroxidase and used to infect cells and then localized by developing the electron-dense tracer (Fig. 5). (iii) Unlabeled virions were used to infect cells, and after fixation, monovalent antibody Fab' fragments labeled with horseradish peroxidase were used to bind and localize the virus when the electron-dense tracer was subsequently developed (Fig. 6).

The result of the optimalization of the conditions of infection and the use of ultrastructural tracers is that a better understanding of the early events of polyoma virus infection has now been obtained. The data suggest that there is a nuclear transport recognition factor(s) present on virions and pseudovirions that is absent in capsids. This factor possibly determines the fate of the virus particle once it initiates attachment to the host cell receptor site. It would appear that this factor is located near the attachment site on the virus since, if present, the cell takes up the virus by monopinocytosis and then rapidly transports it to the outer nuclear membrane for nuclear entry and subsequent uncoating. If the factor is absent, as must be the case with capsids, the virus does not proceed along this specialized pathway, but rather is taken into phagocytotic vesicles and is marked for destruction either by fusion with lysosomes or by disposal outside of the cell. It is interesting to speculate that the monopinocytotic form of penetration is reserved for those virus particles that not only possess the nuclear transport recognition factor(s) but also are able to undergo successful attachment on their threefold axis.

Examination of a geodestix (8) model of polyoma virus demonstrates that the model could easily interact with a cellular receptor site on its fivefold axis or one vertice (Fig. 4A). This form of attachment is a very loose interaction and consequently is reversible and therefore unstable. The virus particle may also directly interact or roll over from the fivefold axis onto a twofold axis or two vertices. Although the twofold axis interaction appears to be tighter than the fivefold axis interaction with the cellular receptor site, it is again unstable and could possibly oscillate back and forth towards the threefold axis direction on either side of the twofold axis. However, from the model it becomes readily apparent that since the virus particle is almost spherical, the face of the model comes in close contact with the surface before a threepoint contact. In fact it is not possible to position the model on a flat surface on the threefold axis, as it will rest on a twofold axis and a face unless the surface below it is depressed slightly. The twofold axis is the most frequently occurring form of attachment at 4°C, as the fluid membrane is very rigid at that temperature, and hence the virus is sterically hindered by its own curvature from interacting with a flat surface on its threefold axis. Consequently, electron micrographs of the virus attached to the cellular receptor sites at 4°C will only result in the virus being seen on its fivefold (Fig. 4A) or twofold axis (Fig. 4B).

At 37°C the situation is quite different; however, the membrane is more fluid and consequently is more flexible. Under these conditions, possibly at the expense of cellular energy, the membrane can flux or undulate just enough to allow the virion to make contact on a threefold axis. Once the threefold axis contact is made, there must be a rapid signal given to initiate penetration. The cell membrane then begins to invaginate more deeply, possibly keeping in close contact with the virion by interacting with the nine remaining vertices of the icosahedron until the virion pinches off from the cell membrane as a monopinocytotic vesicle. The monopinocytotic vesicle is then ready to initiate its journey to the outer nuclear membrane. Since it appears that penetration by monopinocytosis is a prerequisite for transport to the nucleus and subsequent entry, the recognition of a particular viral protein(s) at the cellular receptor site is a very critical step.

Boulanger and Hennache (2) and Lonberg-Holm and Phillipson (23) postulated that the first stage of adenovirus uncoating occurs at the cell membrane, as virus particles that crossed the membrane became susceptible to exogenous nucleases. Experiments performed to determine if polyoma virions were likewise labilized at the cell surface as a first stage of uncoating demonstrated that the virions are not nuclease sensitive (Table 2) as a result of crossing the cell membrane, and hence a distinctively different mechanism of penetration must occur with polyoma virus.

Chardonnet and Dales (5) and Luftig and Weihing (26) have both postulated that micro-

tubules may play a role in nuclear transport during adenovirus infection. However, the electron microscopy studies presented here demonstrated that microfilaments and microtubules are probably not involved in the rapid and specific transport of the monopinocytotic vesicles from the cell surface to the nucleus. Thus the question of how the monopinocytotic vesicles rapidly and specifically migrate to the outer nuclear envelope and then recognize the site for nuclear entry is still open to speculation.

If a portion(s) of the virion coat were removed as a result of crossing the cell membrane, as has been postulated to occur with adenoviruses (4, 23), then electron microscopy autoradiography studies would have demonstrated an accumulation of grains at the cell surface with time. In addition, if uncoating had been a cytoplasmic event or if the virus were rendered into a quasi-intact state as a result of crossing the nuclear membrane, then an increase of grains would have localized at the nuclear membrane with time. However, neither of these cases was observed. Moreover, radioimmunoprecipitation and electron microscopy using Fab' antibody fragments to polyoma virions, SDS-disrupted virions, and capsomeres labeled with horseradish peroxidase demonstrated that the virus does not undergo a detectable change in antigenicity as a result of crossing either the cell membrane or the nuclear membrane.

Since the pseudovirions used for these studies were derived by pooling the light side of the CsCl gradient virion peak and the heavy side of the capsid peak, a spectrum of differences of both the size and the composition of viral DNA was expected. If the presence of the viral DNA itself was involved in the nuclear transport recognition factor(s), these different DNA molecules, due to their heterogeneous composition and size, should impart a spectrum of charge differences contributing to the net charge of the virus if the DNA is involved in the attachment site. Thus one would predict that a spectrum of mobilities in an electrophoretic field would be produced. However, Thorne et al. (41) have previously demonstrated by zone electrophoresis that the virions and capsids have the same mobility. This indicates that the properties of the capsid alone determines the electrophoretic mobility of the virus particle. It may be concluded therefore that the nuclear transport recognition factor(s) is not the presence of the viral DNA per se. However, this does not exclude the cellular histones found associated with the virions.

The surface structure of polyoma virus has been described by Wildy et al. (46), Klug (20), and Finch (9) and was shown to be composed totally of capsomeres. Moreover, the only morphological difference between virions and capsids by negative-stain electron microscopy is the tightness of fit of the capsomeres and the presence of the viral DNA and histones. Thus, if a nuclear transport recognition factor(s) exists it is not morphologically distinguishable. However, several alternative explanations for the factor(s) may exist. For example, the factor may result from the presence or absence of or a change in the proportion of a particular viral-specific protein(s). Moreover, it may result from a conformational change of a protein near the viral attachment site. Another possible alternative is that the host cell histones that have been shown to be present in both virions and pseudovirions and absent in capsids (R. Consigli, J. Zabielski, and R. Weil, submitted for publication; 11) may be the nuclear transport recognition factor(s). Although the histones have been shown to undergo a close association with the DNA replication complex (27), their biological role during the early events of infection prior to DNA replication still remains obscure. In vitro labeling techniques (13, 28) suggest that at least a portion of the histones are exposed to the environment at the surface of the virion in some manner. Wildy et al. (46) demonstrated that each capsomere has a 2.0-nm hole in the center. One possible explanation, therefore, might be that the histones reside on the inside of the virus coat but are able to exert some influence at the attachment site(s), either directly through the holes in the capsomere(s) or indirectly by some form of a conformational change. Recent evidence from this laboratory (McMillen and Consigli, unpublished data) suggest that monovalent Fab' fragments to SDS gel purified histones (V_4–V_7) from polyoma virions are able to efficiently neutralize viral infectivity.

These studies have led to the model in Fig. 8 showing the early events of polyoma virus attachment, penetration and nuclear entry. (1) The virus with the nuclear transport recognition factor(s) interacts on either its fivefold or twofold axis with the host cell receptor site at either 4°C or 37°C; (2) at 37°C the cell membrane undulates beneath the virus just enough to allow contact on its threefold axis and thereby signals penetration, possibly as a result of either direct or indirect histone interaction; (3) the virus penetrates the cell membrane, which closes tightly about the virus particle, thereby pinching it off to form a monopinocytotic vesicle; (4) the monopinocytotic vesicle rapidly and selectively migrates to the outer nuclear membrane; (5) upon contact with the outer nuclear membrane, the virus particle en-

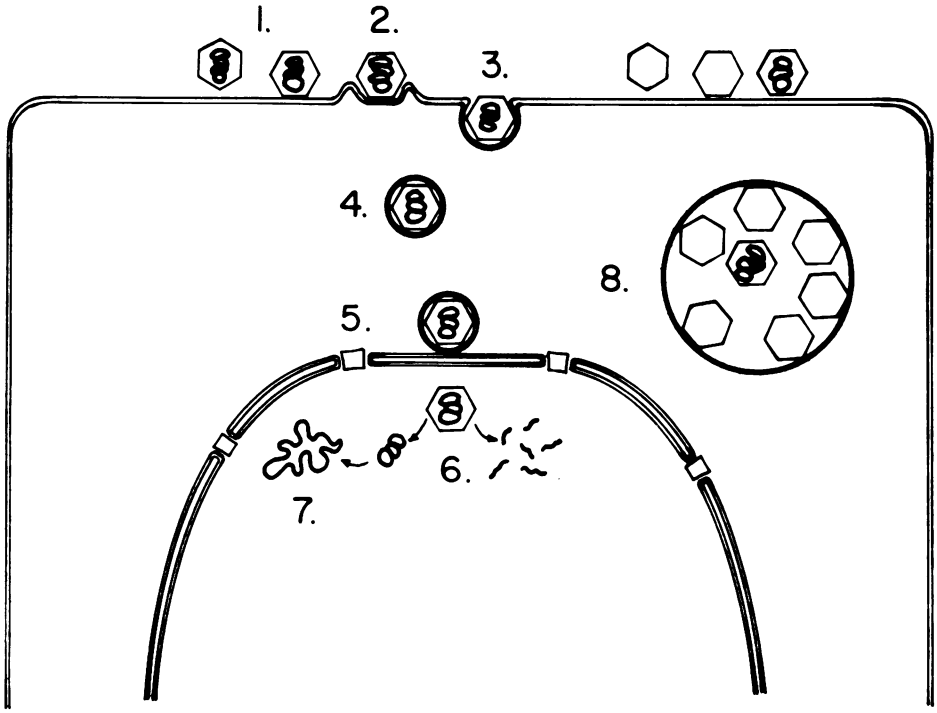

FIG. 8. *Model of polyoma virion attachment, penetration, and nuclear entry (see text for description).*

ters the nucleus devoid of a membrane; (6) once within the nucleus the virus particle is uncoated and the viral DNA is released (7) for transcription and translation of viral genes; (8) capsids appear to enter the cytoplasm in groups within phagocytotic vesicles.

The data presented in this investigation demonstrate that DNA-containing virus particles (virions and pseudovirions) penetrated via a specialized monopinocytotic mechanism, resulting in nuclear transport and entry. On the other hand, non-DNA-containing virus particles (capsids) were religated to penetration within phagocytotic vesicles and were not found to enter the nucleus. It was also demonstrated that the virion DNA and coat proteins simultaneously arrived as early as 15 min postinfection in the nucleus. This indicates that virion uncoating is an event subsequent to nuclear entry. The above findings were found to occur in both permissive and nonpermissive cells infected with purified virions. This indicates that the restrictive event(s) that determines the fate of the productive as well as nonproductive infection occurs subsequent to nuclear entry of the infecting virions.

ACKNOWLEDGMENTS

This investigation was supported by Public Health Service grant CA-07139 from the National Cancer Institute. R. M. was the recipient of a President's Fellowship from the American Society for Microbiology to study with P. K. Nakane, University of Colorado Medical Center, Denver, Colo.

LITERATURE CITED

1. **Benjamin, T. L.** 1972. Physiological and genetic studies of polyoma virus. Curr. Top. Microbiol. Immunol. 59:107-133.
2. **Boulanger, P. A., and B. Hennache.** 1973. Adenovirus uncoating: an additional evidence for the involvement of cell surface in capsid labilization. FEBS Lett. 35:15-18.
3. **Bourgaux, P.** 1964. The fate of polyoma virus in hamster, mouse and human cells. Virology 23:46-55.
4. **Brown, D. T., and B. T. Burlingham.** 1973. Penetration of host cell membranes by adenovirus 2. J. Virol. 12:386-396.
5. **Chardonnet, Y., and S. Dales.** 1972. Early events in the interaction of adenoviruses with HeLa cells. III. Relationship between an ATPase activity in nuclear envelopes and transfer of core material: a hypothesis. Virology 48:342-359.
6. **Consigli, R. A., H. C. Minocha, and H. Abo-Ahmed.** 1966. Multiplication of polyoma virus. II. Source of constituents for viral deoxyribonucleic acid and protein synthesis. J. Bacteriol 92:789-791.
7. **Eddy, B. E., S. E. Stewart, and W. Berkeley.** 1958. Cytopathogenicity in tissue cultures by a tumor virus from mice. Proc. Soc. Exp. Biol. Med. 98:848-851.
8. **Finch, J. T., and A. Klug.** 1965. The structure of viruses of the papilloma-polyoma type. III. Structure of rabbit papilloma virus. J. Mol. Biol. 13:1-12.
9. **Finch, J. T.** 1974. The surface of polyoma virus. J. Gen. Virol. 24:350-364.
10. **Fraser, K. B., and E. M. Crawford.** 1965. Immunoflu-

orescent and electron-microscopic studies of polyoma virus in transformation reaction with BHK 21 cells. Exp. Mol. Pathol. 4:51-65.
11. **Frearson, P. M., and L. V. Crawford.** 1972. Polyoma virus basic proteins. J. Gen. Virol. 14:141-155.
12. **Friedmann, T., and M. Haas.** 1970. Rapid concentration and purification of polyoma virus and SV40 with polyethylene glycol. Virology 42:248-250.
13. **Gibson, W.** 1974. Polyoma virus proteins: a description of the structural proteins of the virion based on polyacrylamide gel electrophoretic analysis. Virology 62:319-336.
14. **Girardi, A. J.** 1959. The use of fluorocarbon for "unmasking" polyoma virus hemagglutinin. Virology 9:488-489.
15. **Graham, R. C., and M. Karnovsky.** 1966. The early stages of adsorption of injected hroseradish peroxidase in the proximal tubules of mouse kidney: ultrastructural cytochemistry by a new technique. J. Histochem. Cytochem. 14:291-302.
16. **Horowitz, M. S., and M. D. Scharff.** 1969. Immunological precipitation of radioactively labeled viral proteins, p. 297-315. *In* K. Habel and N. P. Salzman (ed.), Fundamental techniques in virology. Academic Press Inc., New York.
17. **Kekwick, R. A.** 1940. The serum proteins in multiple myelomatosis. Biochem. J. 34:1248-1257.
18. **Khare, G. P., and R. A. Consigli.** 1965. Multiplication of polyoma virus. I. Use of selectively labeled (^{3}H) virus to follow the course of infection. J. Bacteriol. 90:819-821.
19. **Khare, G. P., and R. A. Consigli.** 1967. Cytologic studies in polyoma virus-infected mouse embryo cells. Am. J. Vet. Res. 28:1527-1536.
20. **Klug, A.** 1965. Structure of viruses of the papilloma-polyoma type. II. Comments on other work. J. Mol. Biol. 11:424-431.
21. **Kopriwa, B. M.** 1973. A reliable, standardized method for ultrastructural electron microscopic radioautography. Histochemie 37:1-17.
22. **Levy, H. B., and H. A. Sober.** 1960. A simple chromatographic method for preparation of gamma globulin. Proc. Soc. Exp. Biol. Med. 103:250-252.
23. **Lonberg-Holm, K., and L. Philipson.** 1969. Early events of virus-cell interaction in an adenovirus system. J. Virol. 4:323-338.
24. **Lowry, O. H., N. J. Rosebrough, A. L. Farr, and R. J. Randall.** 1951. Protein measurements with the Folin phenol reagent. J. Biol. Chem. 193:265-275.
25. **Luft, J. H.** 1961. Improvements in epoxy resin embedding methods. J. Biophys. Biochem. Cytol. 9:409-414.
26. **Luftig, R. B., and R. R. Weihing.** 1975. Adenovirus binds to rat brain microtubules in vitro. J. Virol. 16:696-706.
27. **McMillen, J., and R. A. Consigli.** 1974. Characterization of polyoma DNA protein complexes. I. Electrophoretic identification of the proteins in a nucleoprotein complex isolated from polyoma-infected cells. J. Virol. 14:1326-1336.
28. **McMillen, J., and R. A. Consigli.** 1974. In vitro radioisotopic labeling of proteins associated with purified polyoma virions. J. Virol. 14:1627-1629.
29. **Macpherson, I., and M. Stoker.** 1962. Polyoma transformation of hamster cell clones—an investigation of genetic factors affecting cell components. Virology 16:147-151.
30. **Mattern, C. F., K. K. Takemoto, and W. A. Daniel.** 1966. Replication of polyoma virus in mouse embryo cells: electron microscopic observations. Virology 30:242-256.
31. **Millonig, G.** 1961. Advantages of a phosphate buffer for OsO_4 solutions in fixation. J. Appl. Physiol. 32:1637.
32. **Nakane, P. K.** 1975. Recent progress in the peroxidase-labeled antibody method. Ann. N.Y. Acad. Sci. 254:203-211.
33. **Nakane, P. K., and A. Kawaoi.** 1974. Peroxidase-labeled antibody: a new method of conjugation. J. Histochem. Cytochem. 22:1084-1091.
34. **Puck, T. T., S. J. Cieciura, and A. Robinson.** 1958. Genetics of somatic mammalian cells. III. Long-term cultivation of euploid cells from human and animal subjects. J. Exp. Med. 108:945-956.
35. **Sachs, L., M. Fogel, and E. Winocour.** 1959. In vitro analysis of mammalian tumor virus. Nature (London) 183:663-664.
36. **Sachs, L., and D. Medina.** 1961. In vitro transformation of normal cells by polyoma virus. Nature (London) 189:457-458.
37. **Salpeter, M. M., L. Bachman, and E. E. Salpeter.** 1969. Resolution in electron microscopy autoradiography. J. Cell Biol. 41:1-20.
38. **Shipman, C.** 1969. Evaluation of 4-(2-hydroxyethyl)-1-piperazineethane-sulfonic acid (Hepes) as a tissue culture buffer. Proc. Soc. Exp. Biol. Med. 130:305-310.
39. **Steiner, L. A., and S. Lowey.** 1966. Optical rotatory dispersion studies of rabbit α G-immunoglobulin and its papain fragments. J. Biol. Chem. 241:231-240.
40. **Stoker, M., and P. Abel.** 1962. Conditions affecting transformation by polyoma virus. Cold Spring Harbor Symp. Quant. Biol. 27:375-386.
41. **Thorne, H. V., H. House, and Z. L. Kisch.** 1965. Electrophoretic properties and purification of large and small plaque-forming strains of polyoma virus. Virology 27:37-43.
42. **Tooze, J.** 1973. The lytic cycle of polyoma virus, p. 305-349. *In* J. Tooze (ed.), The molecular biology of tumor viruses. Cold Spring Harbor Press, Cold Spring Harbor, N.Y.
43. **Vinograd, J., and J. E. Hearst.** 1962. Equilibrium sedimentation of macromolecules and viruses in a density gradient. Prog. Chem. Org. Nat. Prod. 20:372-422.
44. **Vogt, M., and R. Dulbecco.** 1960. Virus-cell interaction with a tumor-producing virus. Proc. Natl. Acad. Sci. U.S.A. 46:365-370.
45. **Weil, R., C. Salmon, E. May, and P. May.** 1974. A simplified concept in tumor virology: virus-specific "pleiotrophic effectors." Cold Spring Harbor Symp. Quant. Biol. 39:381-395.
46. **Wildy, P., M. G. P. Stoker, I. A. Macpherson, and R. W. Horne.** 1960. The fine structure of polyoma virus. Virology 11:444-457.